 SDHM, vol.6, no.3, pp.189-212, 2010

Identification of Material Parameters for Structural Analyses

W. Brocks[1] **and I. Scheider**[2]

Abstract: Material parameters are adjustable coefficients in constitutive equations of the mechanical behaviour. Their identification requires a combined experimental and numerical approach, which results in a generally ill-posed inverse problem. Methods commonly applied in computational mechanics like optimisation and neural networks are addressed, and problems like sensitivity, uniqueness and stability are discussed. The cohesive model for describing ductile tearing is chosen as practical example to substantiate the general considerations.

Keywords: parameter identification, optimisation, evolution strategy, neural network, cohesive model.

1 Introduction

The finite element method (FEM) is a well-established, reliable and versatile tool for assessing the structural performance, safety, durability and lifetime. Predictions are based on mathematical models of the mechanical behaviour. The mathematics behind is beyond dispute, it is the physics of the constitutive laws for deformation and damage that governs the reliability of the predictions. In particular, the model parameters play a crucial role, which is regrettably often underrated. Experts of continuum mechanics, who establish sophisticated constitutive equations for advanced applications, frequently consider parameter identification as a practical problem to be executed by material testers. The material scientists in turn tend to distrust computational methods in general and to confuse material characterisation for the experimental determination of so-called material properties independent of any model.

The literature on parameter identification is much less extensive than that on advanced constitutive models. The simulations executed with a certain model appear more intriguing than the question, how the respective material parameters have

[1] Christian Albrecht University Kiel, Germany
[2] Helmholtz-Zentrum Geesthacht, Centre for Material and Coastal Research, Germany

been determined. However, the reliability of structural analyses, which is of vital interest for engineering purposes, depends on the accuracy of the material parameters and can only be improved if the gap between constitutive modelling and testing is reduced. This requires a mutual understanding among the specialists of the respective methods and problems.

The present article aims at contributing to this process by outlining the general principles and methods of parameter identification on the one hand and illustrating the application for a common and comparably simple model of ductile tearing on the other hand. Choosing a more complex constitutive model would just complicate the presentation without any gain of deeper insight.

2 Material Characterisation and Parameter Identification

2.1 Material Parameters - Model Parameters

The notion of what material parameters are has changed in the history together with the expansion of theory and mathematics into strength of materials, which allowed for reducing different phenomena to just different boundary value problems (BVP) governed by the same basic equations, namely deformation kinematics, Cauchy's equation of motion and material specific constitutive equations. Material parameters are only meaningful in the context of the latter, i.e. a model of the mechanical behaviour of a certain material. If this model is simple, e.g. isotropic elasticity or elasto-plasticity, and the stress state is uniaxial, the respective BVP can be solved analytically and the respective material parameters directly evaluated from a mechanical test. Thus the awareness of the catenation between a specific constitutive model and the respective parameters has partly sunk into oblivion.

Material behaviour may be elastic or inelastic, temperature dependent, deformation-rate and time dependent, isotropic or anisotropic. The phenomena are numerous and the number of models proposed in the literature is even larger. The more complex the phenomena are, which are subject to modelling, the more sophisticated the models have to be and the more parameters appear in the models. No analytical solutions can be obtained any more, and due to the complex phenomena to be described, the tests and their evaluation become more and more sophisticated. This is the background of hybrid methods (Brocks and Steglich, 2007), which actually label the synergy between experimental and numerical methods for material characterisation (Mahnken, 2004).

Fracture mechanics has introduced the concept of fracture toughness in terms of stress intensity factor, K, J-Integral, crack-tip opening displacement (CTOD), δ, etc. (see the topical overview by Brocks et al., 2003). There are ongoing discussions if and under which conditions they may be regarded as material parameters.

The theoretical background rests on asymptotic solutions of the stress fields at crack tips in elastic or elasto-plastic bodies. The pivotal question is, whether the fracture toughness measured on test specimens, who are designed to match the underlying theoretical concept, can be used for predicting crack extension in arbitrary engineering structures. The simple answer is, "yes they can" as long as the stress state in the structure resembles the stress state in the test specimen. If this is not checked in practical applications, the predictions will most likely fail.

This problem of transferability dominated the discussions on the applicability of *J*R-curves to ductile tearing for many years and finally promoted local approaches to damage evolution (Lemaitre, 1986). The new constitutive theories came up with new model parameters and evoked the discussion, whether these parameters may be called material properties. On the background of constitutive modelling, this is a pointless question, however. Understanding material parameters just as adjustable coefficients in a certain model, gives up the universal claim of characterising inherent features of a material for the benefit of a more manageable and pragmatic meaning. This perception will be adopted in the following.

2.2 The Identification Problem

The process of material characterisation is mathematically expressed as an inverse problem (Mahnken, 2004, Brocks et al., 2008).

Let $\mathbf{R}(\mathbf{x},t)$ denote the response of a structure in terms of measurable quantities to mechanical or thermal actions, $\mathbf{F}(\mathbf{x},t)$, with $\mathbf{x}$ and t being the coordinates and the time, respectively. The response of an accordant constitutive model can be described by a functional,

$$\mathbf{R}_{\mathrm{mod}}(\mathbf{x},t) = \mathscr{F}_{\tau=0}^{t}\{\mathbb{G},\mathbf{c},\mathbf{F}(\mathbf{x},\tau)\}\,, \tag{1}$$

in dependence on the geometry, $\mathbb{G}$, the material parameters, $\mathbf{c} = \{c_i\}$, and the loading history, $\mathbf{F}(\mathbf{x},t)$. The functional $\mathscr{F}$ is represented by an analytical or numerical solution of an initial boundary value problem (IBVP). It is assumed that this solution is obtained by a finite element (FE) model of the structure. Eq. (1) is addressed as direct problem, where $\mathbb{G}$, $\mathbf{c}$, and $\mathbf{F}$ are the input and $\mathbf{R}_{mod}(\mathbf{x},t)$ is the output in terms of a displacement, strain or stress field, which is recorded in a finite number of geometrical points, $\mathbf{x}_i$, and time steps, t_j.

For material characterisation, the structure is a test specimen that is particularly designed for parameter identification, and hence the geometry, $\mathbb{G}$, and the loading history, $\mathbf{F}$, are determinate and fixed by a test procedure. Assuming that a solution of the direct problem, eq. (1), and a procedure for finding it exists, the functional

mathcalF reduces to a mapping,

$$\mathbb{R}_{\mathrm{c}} \underset{\mathbb{G},\mathbf{F}}{\mapsto} \mathbb{R}_{\mathrm{R}}: \quad \mathbf{R}_{\mathrm{mod}} = \mathscr{R}(\mathbf{c}), \tag{2}$$

with $\mathbf{c} \in \mathbb{R}_{\mathrm{c}}$ and $\mathbf{R}_{\mathrm{mod}} \in \mathbb{R}_{\mathrm{R}}$, the spaces of physically meaningful material parameters and response data, respectively.

The corresponding inverse problem consists of finding the parameter vector, $\mathbf{c}$, for a given experimentally measured response, $\mathbf{R}$,

$$\mathbb{R}_{\mathrm{c}} \underset{\mathbb{G},\mathbf{F}}{\mapsto} \mathbb{R}_{\mathrm{R}}: \quad \mathbf{c} = \mathscr{R}^{-1}(\mathbf{R})\big|_{\mathbb{G},\mathbf{F}(\mathbf{x}_i,t_j)}, \tag{3}$$

(Bolzon et al., 2004, Mahnken, 2004). Mathematically, this implies that the given information allows for a unique solution, i.e. $\mathscr{R}^{-1}$ is unique and $\mathbf{R}$ is complete. In order that the parameters, $\mathbf{c}$, may be called material parameters, i.e. transferable to other structures, $\mathscr{R}^{-1}$ is supposed to be independent of Γ and $\mathbf{F}$. It is assumed, that the numerical calculation yields correct results, i.e. the implementation of the material model is correct, the chosen boundary conditions represent the test conditions and an adequate solution strategy including a reasonable meshing of the structure has been chosen.

Numerous uncertainties interfere with the need for a unique solution, nevertheless.

The measured response contains measuring errors of various kinds, due to the testing procedure and machine, the gauge, imperfections of the specimen geometry, etc.. Random variations of test records can more or less be eliminated by averaging. Systematic errors like offsets or drifts, effects of temperature etc. require a compensation or subsequent adjustment. Response vectors from different kinds of tests may also be weighted in the parameter identification process, according to a subjective ranking of their respective significance.

Another important source of uncertainties is the scattering of material properties. Various tests result in varying responses and will hence be represented by different sets of parameters. As long as the scatter is minor with respect to engineering purposes, mean values are acceptable. Very often only a single test is accomplished and evaluated, anyway. But if scatter is an inherent feature, a sufficient number of tests has to be provided and averaging is improper.

Last but not least, any material model provides an approximate representation of the real behaviour, only. There is hence a systematic deviation between the model response, $\mathbf{R}_{mod}$, and the measured one, $\mathbf{R}$, which can be minimised but never resolved. Increasing the number of parameters in a model in order to improve its predictions is often not advisable as it may result in non-unique solutions.

Uniqueness of material parameters is essential for any transfer to engineering structures, i.e. if the prediction of their respective mechanical behaviour is intended. Non-uniqueness becomes obvious, if the application of the model to another specimen type or loading configuration fails to yield satisfactory results, provided the constitutive model itself is adequate. Hence, it is recommended to provide test data for at least a second case and check the model response.

Missing uniqueness can be due to incomplete data, and additional experiments are then required for the identification procedure. The design of appropriate tests for parameter identification is as important as constitutive modelling itself.

Finally, stability of the solution means that the simulated structural response depends continuously on the parameters. If this condition is not fulfilled, small perturbations in the test data, for example caused by measurement errors, may result in uncontrolled oscillations of the model parameters. This is a model fault and will most likely cause divergence of the optimisation procedure. Though being annoying, this is actually the least dangerous problem of all, as getting no solution is better than getting a wrong one without realising it.

2.3 Optimisation Methods

Apart from manual fitting and trial and error, numerical optimisation techniques are frequently applied, particularly for highly nonlinear models with numerous parameters. They minimise the “error”, i.e. the deviation between model and experimental results with respect to some "target" or "quality function".

$$q(\mathbf{c}) = \|\mathbf{r}(\mathbf{c})\| = \|\mathbf{R}_{\mathrm{mod}}(\mathbf{c}) - R\| \rightarrow \min_{\mathbf{c}\in\mathbb{R}_{\mathbf{c}}} \tag{4}$$

The solution will depend on the choice of the quality function.

The problem can be solved by deterministic or stochastic procedures. Deterministic methods calculate variations of the parameter vector by a unique algorithm, so that the path in the design space is always the same for identical starting vectors, leaving no room for randomness. The advantage of this strategy is a fast convergence for continuous functions. If there is more than one minimum of the target function, the method will find the local minimum next to the starting vector only. Stochastic methods determine variations of the parameter vector by a random generator. They are comparably slow in convergence but better suited for finding the global minimum independent of the starting vector.

In a pure Monte-Carlo search, randomly distributed parameter vectors are generated and that one having the minimum distance to $\mathbf{R}$ according to eq. (4) is taken as an estimate for the optimal parameter vector, $\mathbf{c}^*$. This procedure does not yield

a very good estimate, in general, but can be used for determining a reasonable starting vector in the parameter space.

Using deterministic optimisation methods (Mahnken and Stein, 1994, Bruhns and Anding, 1999) to minimise eq. (4), the optimal vector, $\mathbf{c}^*$, is determined from the necessary condition

$$\nabla q(\mathbf{c}^*) = \mathbf{J}^{\mathrm{T}}(\mathbf{c}^*)\mathbf{r}(\mathbf{c}^*) = \mathbf{0} \tag{5}$$

with $\mathbf{J}$ being the Jacobian. As the residual, $\mathbf{r}(\mathbf{c})$, results from the numerical solution of the IBVP, $\mathbf{J}$ has to be calculated by finite differences. A sequence of parameter vectors $\mathbf{c}_{k+1} = \mathbf{c}_k + \Delta\mathbf{c}_k = \mathbf{c}_k + \alpha_k\mathbf{d}_k$ with $\|\mathbf{r}_{k+1}\| < \|\mathbf{r}_k\|$ is generated, where $\mathbf{d}_k$ is the search direction and α_k is the step length. The search direction can for instance be assumed along the direction of steepest decent, given by

$$\mathbf{d}_k = -\nabla q|_{\mathbf{c}_k} = -\mathbf{J}_k^{\mathrm{T}}\mathbf{r}_k. \tag{6}$$

The search for a minimum point $\mathbf{c}^*$ of eq. (4) is thus reduced to a sequence of one-dimensional optimisation problems (Dennis and Schnabel, 1983).

In general, one may not expect the numerical models to depend smoothly on the parameters and continuous derivatives to exist. The objective function may also exhibit multiple local minima, so that the result of the minimisation process will depend on the starting vector. In these cases, evolutionary algorithms (Schwefel, 1995) provide a way out of this trouble. They include some artificial intelligence and use stochastics combined with search models mimicking natural phenomena, namely genetic inheritance and Darwinian strife for survival. The individuals of nature stand in a sequential competition to each other. Individuals, whose properties are better coordinated with the environment, have an advantage over others. Badly adapted individuals lose the competition and are rejected.

Evolutionary algorithms (Müller and Hartmann, 1989, Furukawa and Yagawa, 1997) maintain a population of individuals, represented by model responses, $\mathbf{R}_{\mathrm{mod}}$, that evolve according to rules of selection, recombination and mutation of their genes, represented by the parameters, $\mathbf{c}$. Each individual of the population receives a measure of its fitness in the environment by means of the target function, eq. (4). Reproduction focuses attention on high fitness individuals. Optimisation can be thought of as an evolution of model responses through various generations.

An evolutionary algorithm is not a random search. It uses stochastic processes, but the result, i.e. the optimal parameter set, is non-random. Due to mutation and recombination, the procedure is non-deterministic, however, and therefore follows a non-unique convergence path. This feature allows finding a global minimum of the target function independent of the choice of the starting point. Various evolutionary

algorithms have been proposed, such as genetic algorithms, evolutionary programming, evolution strategies, genetic programming and classifier systems (Schwefel, 1995). Among the evolutionary algorithms, the evolution strategy became the most prominent representative, which is commonly referred to be the best, i.e. fastest and most efficient, for optimisation tasks.

2.4 Neural Networks

The concept of neural networks (NN) is derived from observations of the information flux between biological neurons. A NN is trained to learn general nonlinear relations. Mathematically it is a nonlinear operator, $\mathscr{N}$, who maps in input vector, $\mathbf{x}$, to an output vector, $\mathbf{y}$, of differing dimensions. In each synapse, incoming information, $x_j^{(n)}$, is multiplied by synaptic weights, $w_{kj}^{(n)}$, and summed up to activations, $v_k^{(n)}$,

$$v_k^{(n)} = \sum_{j=1}^{J_n} w_{kj}^{(n-1)} x_j^{(n-1)} , \quad n = 1, ..., N, \tag{7}$$

which yield the outgoing information, $y_k^{(n)}$, via nonlinear activation functions, $y_k^{(n)} = \varphi_k^{(n)} \left(v_k^{(n)} \right)$. The latter may include thresholds below which no outgoing signal is transmitted. A so-called feed-forward neural network consists of N layers, where the output, $\mathbf{y}^{(n-1)}$, becomes the input, $\mathbf{x}^{(n)}$, of the subsequent layer.

For the purpose of parameter identification, the operator is deployed to solve the inverse problem of eq. (3),

$$\mathbb{R}_\mathrm{R} \mapsto \mathbb{R}_\mathrm{c} : \quad \mathbf{c} = \mathscr{N}(\mathbf{R}), \tag{8}$$

(Ghaboussi, 1991, Sumpter, 1996, Broese and Löffler, 2004), where the input of the first layer is $\mathbf{x}^{(0)} = \mathbf{R}$ and the output of the Nth layer $\mathbf{y}^{(N)} = \mathbf{c}$.

The synaptic weights, $w_{kj}^{(n)}$, represent the degrees of freedom, which are adjusted to a particular BVP defined by a particular test type and constitutive model in order to match the relation between input, $\mathbf{R}$, and output data, $\mathbf{c}$. This is realised by training of the network with the help of simulation results obtained from the model for various parameter sets: $\mathbf{R}_\mathrm{mod} = \mathscr{N}^{-1}(\mathbf{c})$.

NNs are frequently applied in combination with indentation tests to determine parameters of elasto-plastic constitutive equations (Huber et al., 2002, Bolzon et al., 2004). A once trained network can, in principle, provide material parameters $\mathbf{c}$ from test results $\mathbf{R}$ of the same type for all materials being described by the same constitutive model. Thus, local scatter of material data within an inhomogeneous

plate or billet (e.g. Rao et al., 2010) or scatter of properties between different heats can be determined.

NNs do not allow for any quantification of the "quality" of the solution as, e.g., eq. (4).

3 The Cohesive Model of Ductile Tearing

3.1 General Concept

The concept of a cohesive zone for modelling crack extension traces back to Dugdale's strip yield model (Dugdale, 1960) and to Barenblatt's approach of avoiding unrealistic singular stresses at a crack tip (Barenblatt, 1962). Modern phenomenological cohesive models are realised in the context of FE models and describe various kinds of decohesion in a process zone by a relation between surface tractions or cohesive stresses, $\sigma^{\mathrm{T}} = \{\sigma_{\mathrm{n}}, \sigma_{\mathrm{t}}, \sigma_{\mathrm{s}}\}$, having one normal and two tangential components and the material separation, $\delta^{\mathrm{T}} = \{\delta_{\mathrm{n}}, \delta_{\mathrm{t}}, \delta_{\mathrm{s}}\}$, where $\delta = [\mathbf{u}] = \mathbf{u}^{+} - \mathbf{u}^{-}$ is the displacement jump over the interface. Cohesive zones are introduced in finite element meshes as surface elements at the boundaries of solid elements along pre-defined crack paths.

The constitutive relation of the interface elements, the so-called cohesive or, more precisely, decohesion or separation law, $\sigma = \mathbf{f}(\delta)$, which represents the effective mechanical behaviour due to the micromechanical processes of material separation and fracture, cannot be measured directly. Various functions have been proposed and used in the literature (see overview by Brocks et al., 2003), some of which are shown in **Figure 1**.

All these approaches have in common, that stresses reach a maximum, the cohesive strength, σ_c, beyond which they decrease and become zero at some critical separation, δ_c. Alternatively to δ_c, the energy-release rate or separation energy, Γ_c, which represents the area under the traction-separation law,

$$\Gamma_{\mathrm{c}} = \int_0^{\delta_{\mathrm{c}}} \sigma_{\mathrm{n}}(\delta_{\mathrm{n}})\, d\delta_{\mathrm{n}}, \tag{9}$$

can be introduced as a cohesive parameter.

In order to quantify the various shapes, Scheider (2000) proposed a rather versatile

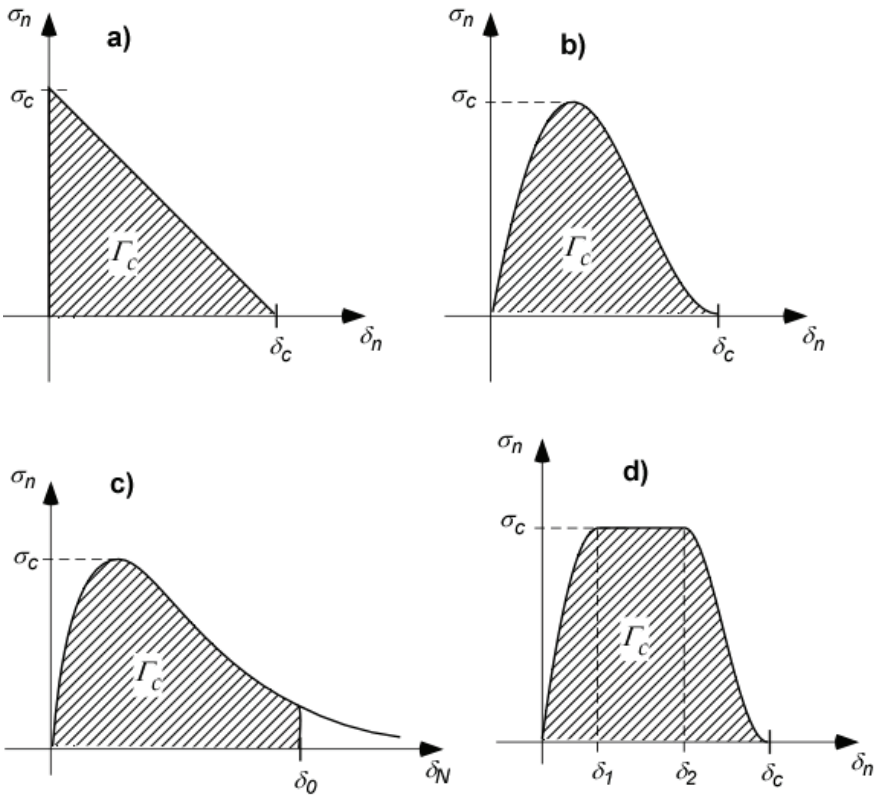

Figure 1: Various separation laws for normal tractions (mode I fracture): a) linearly decreasing (Hillerborg et al., 1976), b) third order polynomial (Needleman, 1987), c) exponential (Needleman, 1990), d) piecewise polynomial with stress plateau (Scheider, 2000).

and steadily differentiable cohesive law for mode I,

$$\sigma_{\mathrm{n}}(\delta_{\mathrm{n}}) = \sigma_{\mathrm{c}} \cdot \begin{cases} 2\left(\frac{\delta_{\mathrm{n}}}{\delta_1}\right) - \left(\frac{\delta_{\mathrm{n}}}{\delta_1}\right)^2 & \text{for } \delta_{\mathrm{n}} \le \delta_1 \\ 1 & \text{for } \delta_1 < \delta_{\mathrm{n}} \le \delta_2 \\ 2\left(\frac{\delta_{\mathrm{n}}-\delta_2}{\delta_{\mathrm{c}}-\delta_2}\right)^3 - 3\left(\frac{\delta_{\mathrm{n}}-\delta_2}{\delta_{\mathrm{c}}-\delta_2}\right)^2 + 1 & \text{for } \delta_2 \le \delta_{\mathrm{n}} \le \delta_{\mathrm{c}} \end{cases} \tag{10}$$

which includes two additional shape parameters, δ_1 and δ_2. The parameter δ_1 should be chosen as small as numerically possible to obtain a high initial stiffness

of the cohesive elements, as the deformation of the structure has to be dominated by the deformation of the solid elements. The parameter δ_2 allows for a variation between deformation controlled, $\delta_2 \to \delta_1$, and an abrupt stress release, $\delta_2 \to \delta_c$, see **Figure 2**, and hence is a third model parameter.

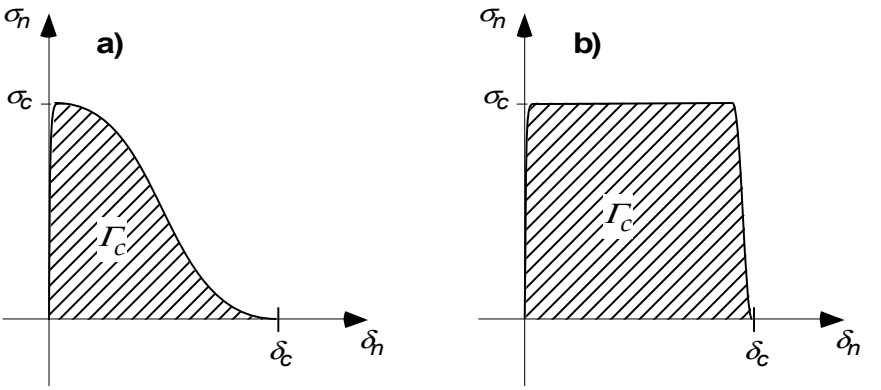

Figure 2: Separation laws according to Eq. (10) for a) $\delta_2 = \delta_1 = 0.01\ \delta_c$, b) $\delta_2 = 0.99\ \delta_c$.

The cohesive law is a phenomenological representation of the mechanisms of damage evolution and material separation on the micro-scale. Evidence on its shape can thus be found from cell models, and the cohesive parameters achieve a micromechanical interpretation (Brocks, 2005). Respective simulations have been performed by Broberg (1997), Siegmund and Brocks (2000), Scheider (2009) for ductile tearing of metals controlled by void nucleation, growth and coalescence, and by Tijssens (2000) for brittle fracture of cementitious materials and crazing of polymers, respectively.

3.2 Effect of the Shape

The effect of the shape of the separation law on the macroscopic mechanical behaviour is still discussed controversially in the literature though there is a general consent that macroscopically brittle (elastic) fracture of ceramics and rock is best described by a linearly decreasing traction-separation behaviour like in **Figure 1a** whereas ductile tearing of metals involving plasticity goes along with a stress plateau like in **Figure 1d**.

Hillerborg et al. (1976) applied a cohesive model with a linearly decreasing separation function as shown in **Figure 1a** to the fracture of concrete. The pseudo R-curve behaviour of concrete due to aggregates has later been incorporated by a bilinearly

decreasing function, see e.g. Petersson (1981), Maier et al. (2006). Quasi-brittle fracture of lamellar γTiAl was successfully modelled by Kabir et al. (2007) using a cohesive law according to eq. (10) with $\delta_2 \approx \delta_1$ as in **Figure 2a**. Lin (1998) simulated ductile crack growth by a Dugdale-type cohesive law similar to **Figure 2b**.

Petersson (1981) presented the first comparative investigation on various cohesive laws, distinguishing between linearly decreasing, Dugdale–type and two different bilinearly decreasing models for plain and fibre reinforced concrete, respectively. Elices et al. (2002) studied three different materials, namely concrete, PMMA and steel with three different shapes of the cohesive law and concluded that the traction-separation law must be chosen in dependence on the class of materials. An analytical study of a block-peel test with an ideally rigid bulk material by Volokh (2004) also revealed that the shape of the separation law is important.

A contradictory and hence frequently cited statement by Tvergaard and Hutchinson (1992) that the shape of the separation law is of minor importance rests upon simulations of linear elastic fracture by a trilinear function similar to **Figure 1d** with varying shape parameters δ_1 and δ_2. Due to the restrictions of this investigation the conclusion may not be generalised. Alfano (2006) compared bilinear, linear-parabolic, exponential and trapezoidal separation laws and concludes that whether or not the shape has an important effect may depend on the boundary value problem and, in particular, on the ratio between the interface toughness and the stiffness of the bulk material. Numerical studies on ductile crack extension in C(T) and M(T) specimens by Scheider and Brocks (2003) substantiate an effect of the shape of the separation law on the crack growth resistance (R-curve) depending on the specimen geometry. In addition to the effect on R-curves, Li and Chandra (2003) found an influence on the size of the plastic zone at the crack tip.

The preceding overview shows that generalising statements on the effect of the shape of the separation law are unhelpful as they may turn out to be either trivial or improper. Respective investigations have to consider and distinguish between specific classes of materials and they should particularly include studies on different specimen geometries considering the problem of transferability. Last but not least, it has to be noted that the shape of the separation law affects the numerical performance of the model (Alfano, 2006).

Micromechanical studies on damage evolution in elastic-plastic materials (Broberg, 1997, Siegmund and Brocks, 2000, Scheider, 2009) as well as simulations of ductile crack extension support the introduction of a stress plateau into the cohesive law as in **Figure 1d**. Its width can be quantified by the shape parameter δ_2, if eq. (10) is adopted. The determination of appropriate values of δ_2 would require systematic numerical and experimental studies on various specimen geometries and on the

transferability of the cohesive parameters in dependence on δ_2. This is actually an open issue. Numerical performance is an additional criterion, as large values $\delta_2 \to 1$ may derogate the convergence.

Numerical simulations of crack extension in aluminium sheet metal (Scheider et al., 2006, Brocks and Scheider, 2007, Scheider and Brocks, 2008) have been successfully performed with a value of $\delta_2 = 0.5\ \delta_c$. which will also be used in the following examples. Thus, the model includes just two parameters, namely cohesive strength, σ_c, and critical separation, δ_c, or cohesive energy, Γ_c, alternatively, which is particularly beneficial for providing an insight into the identification process and its problems.

3.3 Identification Process

The cohesive parameters controlling crack extension are identified on standard fracture mechanics specimens like centre cracked panels, M(T), and compact specimens, C(T), as well as a Kahn-specimen. The latter has been proposed by Kaufmann & Knoll (1964) as a simple test configuration to measure fracture toughness of aluminium alloy sheets. It was first adopted to identify cohesive parameters by Chabanet et al. (2003).

Global quantities like force, F, and load point or load line displacement, V, and local quantities like CTOD, δ, and crack extension, Δa, are monitored in the tests and in the simulations. Their values, i.e. either a global load-displacement curve, $F(V)$, or a resistance curve (R-curve), $\delta(\Delta a)$ or $J(\Delta a)$, are taken to calculate the quality function according to eq. (4). Crack resistance will be denoted as $R(\Delta a)$ in the following, which has the meaning of either measure, J or δ, not to be mistaken for the symbol $\mathbf{R}$ used above to generally denote the response of the system. Thus we have

$$q = \sqrt{\frac{1}{V_{\text{end}}} \int_0^{V_{\text{end}}} \left(\frac{F_{\text{mod}}(V) - F(V)}{F(V)} \right)^2 \mathrm{d}V} \tag{11a}$$

or

$$q = \sqrt{\frac{1}{\Delta a_{\text{end}}} \int_0^{\Delta a_{\text{end}}} \left(\frac{R_{\text{mod}}(\Delta a) - R(\Delta a)}{R(\Delta a)} \right)^2 \mathrm{d}a}. \tag{11b}$$

As the curves are monitored as discrete data points, the integration has to be performed numerically. Obviously, test and numerical results, F and R, have to be

assigned to identical arguments, V or Δa, respectively. If the data are reduced to m equidistantly distributed points the quality function can be calculated by

$$q = \sqrt{\frac{1}{m}\sum_{i=1}^{m}\left(\frac{F_i^{\mathrm{mod}} - F_i}{F_i}\right)^2}\,,\; F_i = F(V_i) \tag{12a}$$

or

$$q = \sqrt{\frac{1}{m}\sum_{i=1}^{m}\left(\frac{R_i^{\mathrm{mod}} - R_i}{R_i}\right)^2}\,,\; R_i = R(\Delta a_i). \tag{12b}$$

For NNs, the complete curve can never be used but must always be reduced to a few data points, which form an input vector of length n:

$$\begin{aligned} \mathbf{x} &= \{F_1, F_2, \ldots, F_n\}\,, \quad \text{or} \\ \mathbf{x} &= \{R_1, R_2, \ldots, R_n\} \end{aligned} \tag{13}$$

Though the data points do not necessarily have to be equidistant, it is nevertheless advisable in order not to weight some regions of the curve more than others - unless this is done on purpose.

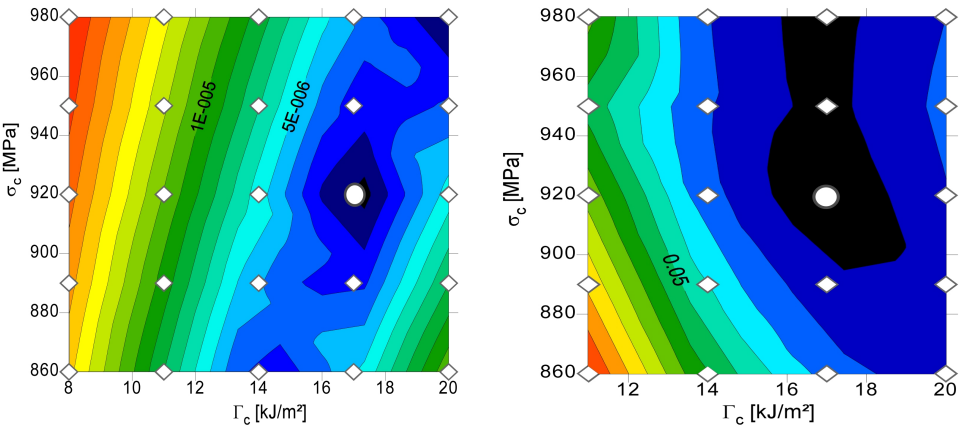

(a) (b)

Figure 3: Quality function q calculated based on $F(V)$ data; (a) for an M(T) specimen, (b) for a Kahn specimen.

In a numerical study, the differences in the error estimation of a structural response using either eq. (11a) or (11b) have been investigated. Crack propagation in different fracture specimens made of a high strength aluminium sheet has been simulated by plane-stress models with varying cohesive parameters $\{\sigma_c; \Gamma_c\}$. The parameters ranges were $\sigma_c \in [860; 980]$ MPa and $\Gamma_c \in [8; 20]$ kJ/m^2. The reference result in this study is no experiment but the simulation with the parameter set {920 MPa; 17 kJ/m^2} (indicated by in the following Figures), i.e. the error for the respective simulation is 0. The intention of this study was to evaluate the uniqueness of the cohesive parameters. The quality functions calculated with the $F(V)$ data and $m = 4$ in eq. (12a) are displayed in **Figure 3**, namely for an M(T) panel in **Figure 3a** and for a Kahn specimen in **Figure 3b**.

It is visible that in both cases the minimum does not have the shape of a bowl but rather of an elongated valley, which is even more pronounced for the Kahn specimen than for the M(T). This clearly indicates that the parameters cannot be identified uniquely based on global mechanical quantities remote from the crack tip. Similar results are reported by Maier et al. (2006).

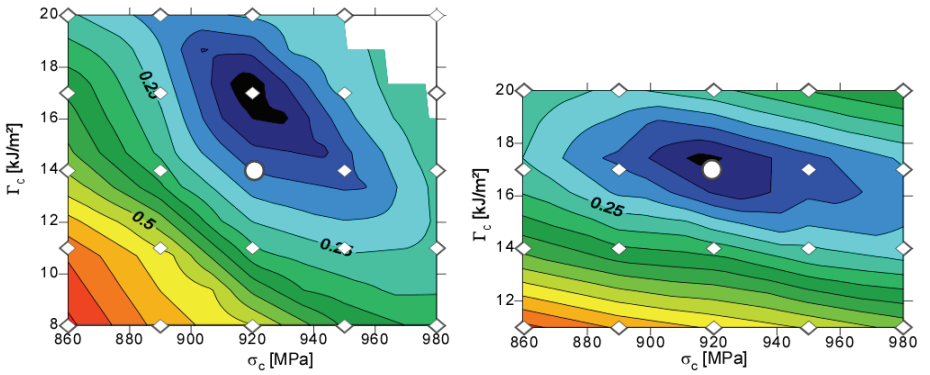

Figure 4: Quality function q calculated based on an R-curve; (a) for an M(T) specimen, (b) for a Kahn specimen.

If an R-curve based on at least one local quantity, Δa, is taken instead, the error contours have a distinct minimum as displayed in **Figure 4**, again for the M(T) panel (a) and for the Kahn specimen (b).

These results prove that only near-field data, particularly R-curves are suited for parameter identification.

In daily routine nevertheless, parameter identification might be performed based on force-displacement curves, since this data can easily be measured whereas more

effort is necessary to obtain an R-curve. The following example shall therefore display the possible error which is made during a parameter identification using experimental $F(V)$ data of a Kahn specimen made of Al 2024 used for airplane fuselages. The reason for taking a Kahn-type specimen was due to the curved structure of the fuselage, which did not allow for manufacturing a larger flat panel.

Three different procedures have been applied, namely an evolution strategy, different gradient optimisation methods and a NN. Two of these strategies, the evolutionary algorithm and the NN, are reported in Brocks et al. (2008). A Python programming environment has been used for the optimisation using the SciPy library package[1] for mathematical and scientific programming. It includes several routines for constrained optimisation, from which the following three were used:

fmin_l_bfgs_b: The L-BFGS-B constrained optimiser by Zhu, Byrd, and Nocedal

fmin_tnc: Truncated Newton Code originally written by Stephen Nash and adapted to C by Jean-Sebastien Roy.

fmin_cobyla: Constrained Optimization BY Linear Approximation

The results are displayed in **Figure 5** for the NN and the gradient methods. Again, the first striking result is that there is no unique minimum, Secondly, the three gradient algorithms yield different minima due to different step sizes and gradient calculations though all processes started from the same initial vector, σ_c = 480 MPa, δ_c = 0.08 mm. In particular, the cobyla algorithm, which uses a gradient in the very first iteration only and then approaches the minimum with finite steps within a trusted region, pointed in a direction quite different from to the two other algorithms, which calculate the gradient in each time step and use larger step sizes.

The NN yields a point which is also located in the valley of minimum error. The training results can be used to generate the contour plot of the quality function, q, in **Figure 5**, since the whole parameter plane is scanned using 30 simulations in the range δ_c = [0.04; 0.20] mm and σ_c = [470; 570] MPa.

The results of the evolution algorithm, which are not displayed in **Figure 5** for clarity, also indicate that the minimum is stretched, since 5 out of 8 individuals of the 41st generation are located along the valley (Brocks et al., 2008). The generic algorithm allows generating a quality surface from all performed simulations. As a gradient algorithm proceeds only along a specific direction and does not scan the whole parameter plane, such a plot cannot be obtained by this method. However, a sensitivity analysis at the optimum can be performed, since gradient information is available.

[1] http://www.scipy.org

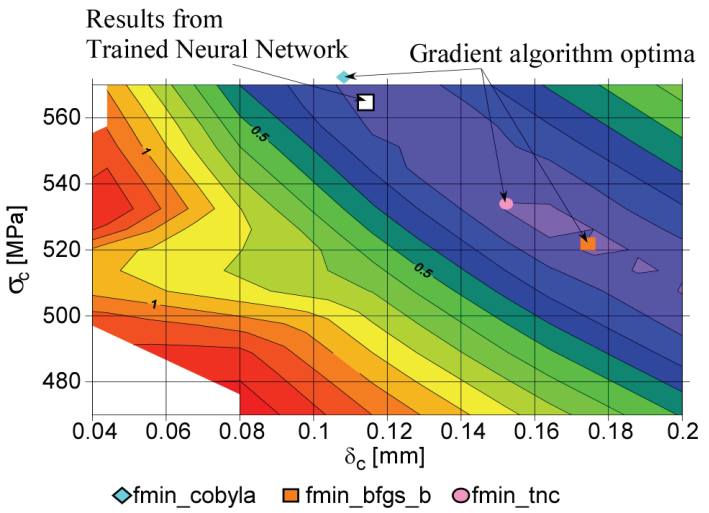

Figure 5: Quality function q calculated based on $F(V)$ data of a Kahn specimen made of Al 2024 and optimisation results from different algorithms.

3.4 Transferability

As pointed out in section 2.2 already, a numerical model is only useful, if the parameters identified from small specimens can be transferred to real large-scale structures, at least within well defined limits of application.

Two main questions have therefore to be answered:

(i) Which specimen should be used to identify a reliable and unique set of parameters, so that the transferability from the specimen used for parameter identification to the structure is ensured?

(ii) Where are the limits for transferability in general?

One important issue, which is often addressed in the literature with respect to the latter question is whether the assumption of constant and unique cohesive parameters is sufficiently accurate for precracked structures under either plane stress or plane strain, see e.g. Siegmund and Brocks (1998), Banerjee and Manivasagam (2009).

The following example investigates the alloy Al 5083 H321, which is mainly used in shipbuilding and automotive industry. Many different experiments on pre-cracked and uncracked sheets (thickness t = 3 mm) have been performed, in particular:

- smooth and notched flat bars,
- C(T) specimens with W = 50, 150 and 1000 mm,
- M(T) specimens with $2W$ = 100 and 300 mm,
- Biaxial loaded cruciform specimen under various load ratios.

Plane-stress crack-propagation analyses using the cohesive model have been performed on these specimens as reported in Scheider et al. (2006) and Brocks et al. (2007). In these investigations, parameter identification was based on trial and error, which depending on the experience of the user leads to good results but needs a large amount of user interaction and cannot be executed automatically. In the following, the determination of parameters will be approached from a different point of view, addressing mainly the question of transferability of the parameters and trying to answer the question, which specimen to use for identification.

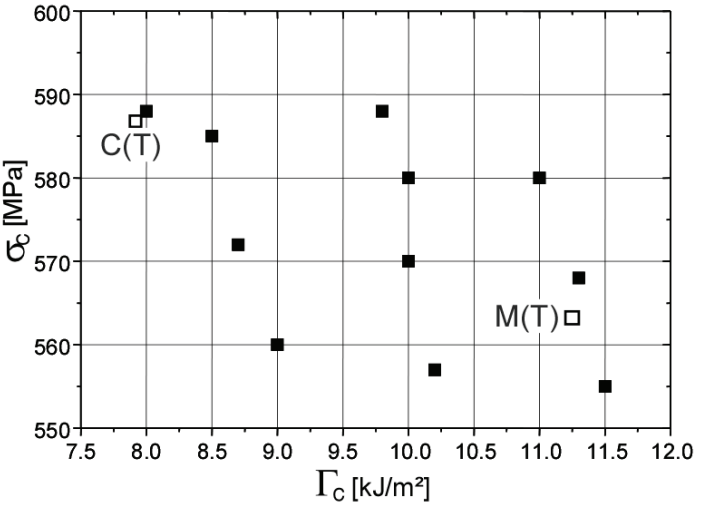

Figure 6: Training matrix and final results for M(T) and C(T) specimen of Al 5083.

According to the previous results, only R-curves should be used. From the previous investigations it was known that an adequate parameter set is given by $\sigma_c = 560$ MPa and $\Gamma_c = 10$ kJ/m^2, using the traction-separation law of eq. (11) with $\delta_2 = 0.5\delta_c$. Here, a more detailed analysis of the identification will be presented. For this purpose NNs have been trained separately for a C(T) and an M(T) specimen. The training range is Γ_c = [8; 11.5] kJ/m^2 and σ_c = [550; 590] MPa and 11 simulations

have been performed for each specimen. After training of the NN with an input vector containing four CTOD values at Δa = 1, 3, 5 and 7 mm the respective experimental R-curves were fed into the network. It turned out that the results for C(T) and M(T) specimen differ by some amount both with respect to cohesive strength and energy, see **Figure 6**, where the final values for both specimens (hollow symbols) and the training matrix (solid symbols) are shown in the parameter plane. One can see that the C(T) has a higher cohesive strength but lower cohesive energy compared to the M(T) specimen. This is in accordance with other investigations, which indicate that a C(T) specimen has a higher stress triaxiality at the crack tip than the M(T) specimen. As shown e.g. in Scheider et al. (2010), this leads to increasing cohesive strength and decreasing cohesive energy.

However, even though a discrepancy between the parameters of the two specimen geometries exists, the questions remain: (i) Does this difference significantly affect the transferability for engineering purposes, and (ii) which of these specimens should be used for parameter identification? As an answer to the first question, each specimen has been simulated using the optimum parameter set of the respective other one. The resulting R-curves together with results of previous simulations using the originally published parameter set (σ_c = 560 MPa, Γ_c =10 kJ/m^2) are presented in **Figure 7**. First of all, one can see that the differences between all curves are less than 10% of their absolute values. Even though the simulation with parameters specifically optimised for the respective specimen fits the experimental results best, marked by symbols, the two other curves lie close as well. The original set identified by trial and error represents a reasonable compromise for both specimen types. If safety is of major concern, one might argue that a lower R-curve which is obtained with the C(T) specimen yields conservative results, but the differences are too small to be generalised.

Calculating the quality function in the whole range of cohesive parameters for both specimens will be illustrative. The contour plots are shown in **Figure 8a** for the C(T) and **Figure 8b** for the M(T) specimen. The parameter set identified by the NN is indicated by the symbol. The NN yielded reasonable results in both cases, but more important is the fact that the minimum for the C(T) forms a valley again, whereas it is more clearly distinct for the M(T). This is similar to the results in the previous section, where the minimum for the Kahn specimen in **Figure 4a** is more stretched than for the M(T) specimen in **Figure 4b**.

The dependence of the cohesive parameters on the stress triaxiality (Siegmund and Brocks, 1999, Anvari et al., 2006, Banerjee and Manivasagam, 2009) is not further delineated here, mainly because the effect is marginal under engineering aspects in the plane-stress examples presented above. What should be kept in mind, however, is that the cohesive parameters will emerge as different in plane stress, plane strain

and three-dimensional models (Scheider and Brocks, 2008), i.e. for thin and thick structures, respectively.

4 Summary and Conclusions

The identification of material parameters in constitutive equations requires a combined experimental and numerical approach, which results in a generally ill-posed

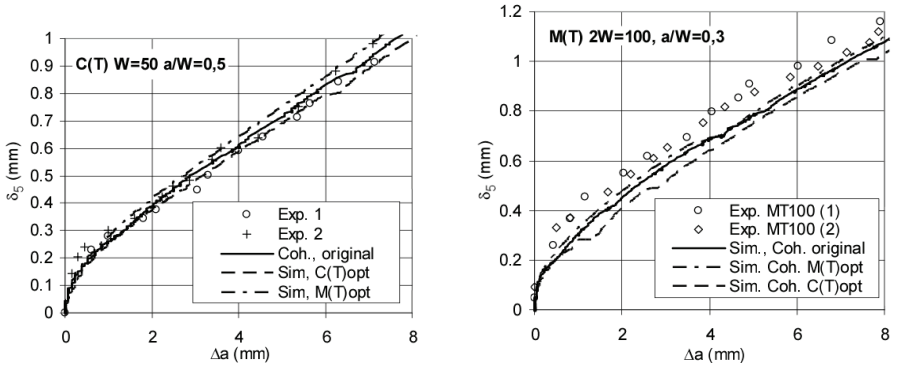

Figure 7: R-curves for pre-cracked specimens made of Al 5083; (a) C(T), (b) M(T). Each subfigure contains the experiments and the numerical results with parameters published by Scheider et al. (2006) and values specifically optimised for the C(T) and the M(T) specimen.

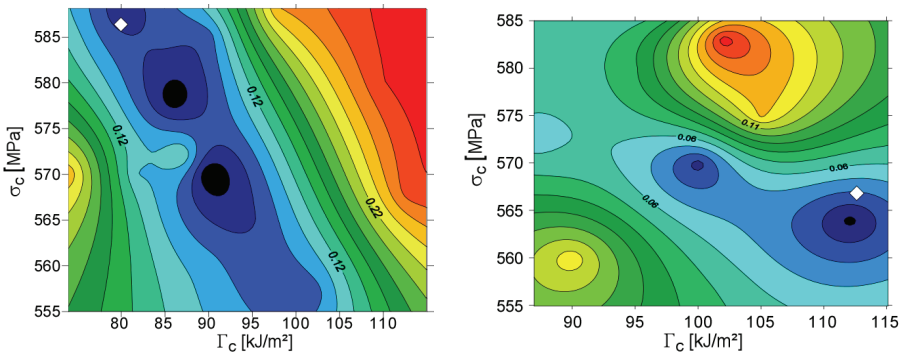

Figure 8: Contour plot of the quality function for different specimens; (a): C(T); (b): M(T). The parameter set obtained by NN is indicated by the white diamond.

inverse problem. Methods commonly applied in computational mechanics, namely optimisation procedures and neural networks have been described and applied to determine cohesive strength and energy. The examples treat ductile crack extension in thin aluminium sheets, which is simulated under the assumption of plane-stress states. Evaluation of a quality (or error) function quantifying deviations between simulation results and a reference solution, commonly obtained from testing, provide useful information on appropriate specimen geometries and measuring data suited for parameter identification. Based on the results described above, the following conclusions can be drawn:

- Data of the crack-tip near-field like CTOD and crack extension, Δa, is more significant for identifying unique values of cohesive parameters than far-field data. Thus R-curves are recommended for parameter identification rather than global load-displacement curves.
- Large crack extension is beneficial for an easier evaluation and significance of an R-curve.
- Though the Kahn-specimen is attractive for being a simple and inexpensive test configuration for sheet metal it is poorly suited for the identification of cohesive parameters.
- It appeared that tensile specimens like M(T) display a more distinct minimum of the quality function than specimens with a high bending fraction. Tensile specimens tend toward numerical instabilities in the simulations on the other hand. Training of a NN which requires scanning of a larger parameter region may hence encounter convergence problems.
- As training has to be executed just once, NNs are specifically suited if a number of different tests is to be evaluated in order to determine variations of material parameters. They do not per se provide any quantification of the "quality" of the solution; an error function may be defined however, if a reference solution is available, and evaluated ex post based on the simulations performed for the training.
- Unlike gradient methods, evolutionary algorithms follow non-unique optimisation paths. This feature allows finding a global minimum of the quality function independent of the choice of the starting point.

References

Alfano, G. (2006): On the influence of the shape of the interface law on the application of cohesive-zone models. *Composites Science and Technology*, vol. 66, pp.

723-730.

Anvari, M.; Scheider, I.; Thaulow, C. (2006): Simulation of dynamic ductile crack growth using strain-rate and triaxiality dependent cohesive elements, *Engng. Fract. Mech*., vol. 73, pp. 2210-2228.

Bäck, T. (1996): *Evolutionary algorithms in theory and practice*, Oxford Univ. Press, Oxford.

Banerjee, A., Manivasagam, R. (2009) Triaxiality dependent cohesive zone model. Eng. Fract. Mech., vol. 76, pp. 1761-1770.

Barenblatt, G.I. (1962): The mathematical theory of equilibrium cracks in brittle fracture. *Advances in Applied Mechanics*, vol. 7, pp. 55-129.

Bolzon, G.; Maier, G.; Panico, M. (2004): Material model calibration by indentation, imprint mapping and inverse analysis". *Int J Solids Struct*, vol. 41, pp. 2957-2975.

Broberg, K.B. (1997): The cell model of materials, *Comput. Mech*., vol.19, pp. 447-452.

Brocks, W. (2005): Cohesive strength and separation energy as characteristic parameters of fracture toughness and their relation to micromechanics. *Struc. Int Durab*, vol.1, pp. 233-244.

Brocks, W.; Cornec, A.; Scheider, I. (2003): Computational aspects of nonlinear fracture mechanics. In: I. Milne, O. Ritchie, B. Karihaloo, (eds.): *Comprehensive Structural Integrity. Fracture of Materials from Nano to Macro*, vol. 3, Elsevier, Oxford, pp. 127-209.

Brocks, W.; Scheider, I.; Schödel, M. (2007): Simulation of crack extension in shell structures and prediction of residual strength. *Arch Appl. Mech.* 76: 655-665.

Brocks, W.; Scheider, I. (2007): Prediction of Crack Path Bifurcation under Quasi-Static Loading by the Cohesive Model. *Struct Durab & Health Monit,* vol. 3, pp. 69-79.

Brocks, W.; Scheider, I.; Steglich, D. (2008): Hybrid methods for material characterisation. *Int J Pure and Appl Math*, vol. 49, pp. 55 558

Brocks, W.; Steglich, D. (2007): Hybrid methods. In: I. Milne, O. Ritchie, B. Karihaloo, B (eds.): *Comprehensive Structural Integrity. Fracture of Materials from Nano to Macro*, vol. 11, Elsevier, Oxford, pp. 107-136.

Broese, E.; Löffler, H.-U. (2004): Artificial neural networks. In: Raabe, D., Roters, F., Barlat, F., Chen, L.-Q. (eds.): *Continuum Scale Simulation of Engineering Materials,* Wiley-VCH, Weinheim, pp. 185-199.

Bruhns, O.T.; Anding D.K. (1999): On the simultaneous estimation of model pa-

rameters used in constitutive laws for inelastic material behaviour. *Int. J. Plasticity*, vol. 15, pp. 1311-1340.

Chabanet, O.; Steglich, D.; Besson, J.; Heitmann, V.; Hellmann, D.; Brocks, W. (2003): Predicting crack growth resistance of aluminium sheets, *Comp Mat Sci*, vol. 26, pp. 1-12.

Cornec, A.; Scheider, I.; Schwalbe, K.H. (2003): On the practical application of the cohesive model. *Engng Fract Mech*, vol. 70, pp. 1963-1987.

Dugdale, D.S. (1960): Yielding of steel sheets containing slits. *J Mech Phys Solids*, vol. 8, pp. 100-104.

Dennis, J.E.; Schnabel, R.B. (1983): Numerical methods for unconstrained optimization and nonlinear equations. Prentice Hall, Englewood Cliffs.

Elices, M; Guinea, G.V., Gómez, J., Planas, J. (2002) The cohesive zone model: advantages, limitations and challenges. *Eng. Fract. Mech*., vol. 69, pp. 137-162.

Furukawa, T.; Yagawa, G. (1997): Inelastic constitutive parameter identification using an evolutionary algorithm with continuous individuals. *Int J Numer Meth Eng*, Vol. 40, pp. 1071-1090.

Furukawa, T.; Yagawa, G. (1998): Implicit constitutive modelling for viscoplasticity using neural networks. *Int J Numer Meth Eng*, vol. 43, pp. 195-219.

Ghaboussi, J. (1991): Knowledge-based modeling of material behavior with neural networks. *J Engng Mech ASCE*, vol. 117, pp. 132-153.

Hillerborg, A.; Modeer, M.; Petersson, P.E. (1976): Analysis of crack formation and crack growth in concrete by means of fracture mechanics and finite elements, *Cement Concrete Res*, vol 6, pp. 773-782.

Huber, N.; Nix, W.D.; Gao, H. (2002): Identification of elastic-plastic materials parameters from pyramidal indentation of thin films. *Proc R Soc London, Ser. A: Math Phys Eng Sci*,, vol 459, pp. 1593-1620.

Kabir, R.M., Cornec, A.; Brocks, W. (2007): Simulation of quasi-brittle fracture of lamellar γTiAl using the cohesive model and a stochastic approach. *Comput. Mater. Sci.,*vol. 39, pp. 75-84

Kaufman, J.; Knoll, A. (1964): Kahn-type tear tests and crack toughness of aluminium alloy sheets. *Materials Research and Standards*, vol. 4, pp. 151-155.

Lemaitre, J. (1986): Local approach of fracture. *Engng Fract Mech*, vol 25, pp. 523-227.

Li, H.; Chandra, N. (2003): Analysis of crack growth and crack-tip plasticity in ductile materials using cohesive zone models. *Int. J. Plast.,* vol. 19, pp. 849-882.

Lin, G. (1998): Numerical investigation of crack growth behaviour using a co-

hesive zone model, PhD thesis, TU Hamburg-Harburg, Germany, Report GKSS 98/E/8, GKSS Research Centre Geesthacht, Germany.

Mahnken, R. (2004): Identification of material parameters for constitutive equations. In: E. Stein, R. de Borst, Th.J.R. Hughes (eds.): *Encycopedia of Computational Mechanics*, Wiley, Chichester, pp. 637–655.

Mahnken, R.; Stein, E. (1994): The parameter identification of viscoplastic models via finite-element-methods and gradient methods. *Model Simulation Mat Sci Eng*, vol. 2, pp. 597-616.

Maier, G., Bocciarelli, M., Bolzon, G., Fedele, R. (2006): Inverse analyses in fracture mechanics. *Int J Fract*, vol. 138, pp. 47-73.

Müller, D.; Hartmann, G. (1989): Identification of material parameters for inelastic constitutive models using principles of biologic evolution. *J Eng Mat Tech*, vol. 111, 299-305.

Needleman, A. (1987): A continuum model for void nucleation by inclusion debonding, *J. Appl. Mech.*, vol. 54, pp. 525-531.

Needleman, A. (1990): An analysis of decohesion along an imperfect interface, *Int. J. Fract.*, vol. 42, pp. 21-40.

Petersson, P.-E. (1981): Crack growth and development of fracture zones in plain concrete and similar materials. PhD thesis, Lund Institute of Technology, Sweden. Report TVBM-1006.

Rao, D.; J. Heerens, J.; Alves Pinheiro, G.; dos Santos, J.F.; Huber, N. (2010): On characterisation of local stress–strain properties in friction stir welded aluminium AA 5083 sheets using micro-tensile specimen testing and instrumented indentation technique. *Mat Sci Eng A*, in press.

Scheider, I. (2000): Simulation of cup-cone fracture in round bars using the cohesive zone model. In: K.J.Bathe (ed.): *Proc. 1st MIT Conf. Computational Fluid and Solid Mechanics*, pp. 460-462.

Scheider, I. (2009): Derivation of separation laws for cohesive models in the course of ductile fracture. *Eng. Fract. Mech.*, vol. 76, pp. 252-263.

Scheider, I.; Brocks, W. (2003): The effect of the traction separation law on the results of cohesive zone crack propagation analyses. *Key Engineering Materials*, vol. 251-252, pp. 313-318.

Scheider, I.; Brocks, W. (2008): Residual strength prediction of a complex structure using crack extension analyses. *Engng Fract Mech*, vol. 75, pp. 4001-4017.

Scheider, I.; Rajendran, M.; Banerjee, A. (2010): Comparison of different stress-state dependent cohesive zone models applied to thin-walled structures. *Engng Fract Mech*, doi:10.1016/j.engfracmech.2010.05.003 (in press).

Scheider, I.; Schödel, M.; Brocks, W.; Schönfeld, W. (2006): Crack propagation analyses with CTOA and cohesive model: Comparison and experimental validation. *Engng Fract Mech*, vol. 73, pp. 252-263.

Schwalbe, K.-H.; Scheider, I.; Cornec, A. (2009): The SIAM method for applying cohesive models to the damage bahaviour of engineering materials and structures. *Report GKSS 2009/1*, GKSS Research Centre Geesthacht, Germany.

Schwefel, H.P. (1995): Evolution and optimum seeking, Wiley-Interscience, New York.

Siegmund, T.; Brocks, W. (1998): The role of cohesive strength and separation energy for modeling of ductile fracture. In: K.L. Jerina and P.C. Paris, (eds) *Proc. 30th Nat. Symp. on Fatigue and Fracture Mechanics*, ASTM STP 1360, American Society for Testing and Materials, Philadelphia, pp. 139-51.

Siegmund, T.; Brocks, W. (1999): Prediction of the work of separation and implications to modeling. *Int. J. Fracture*, vol. 99, pp. 97-116.

Siegmund, T.; Brocks, W. (2000): A numerical study on the correlation between the work of separation and the dissipation rate in ductile fracture. *Engng. Fract. Mech.*, vol. 67, pp. 139-154.

Sumpter, B.G (1996): On the design, analysis, and characterization of materials using computational neural networks. *Ann Rev Mat Sci*, vol. 26, pp. 223-277.

Tijssens, M.G.A. (2000): On the cohesive surface methodology for fracture of brittle heterogeneous solids, PhD thesis, TU Delft, Netherlands, Shaker Publ. B.V., ISBN 90-423-0129-S.

Volokh, K.Y. (2004): Comparison between cohesive zone models. *Communications in Numerical Methods in Engineering*, vol. 20, pp. 845-856.